Modulation Instability of Optical Waves in the Cubic-Quintic Complex Ginzburg-Landau Equation with Fourth-Order Dispersion and Gain Terms

Woo-Pyo Hong and Seoung-Hwan Park

Department of Physics, Catholic University of Daegu, Hayang, Kyongsan, Kyungbuk 712-702, South Korea

Reprint requests to Dr. W.-P. H.; E-mail: wphong@mail.cu.ac.kr

Z. Naturforsch. **59a,** 437 – 442 (2004); received January 5, 2004

The modulation instability of the one-dimensional cubic-quintic complex Ginzburg-Landau equation with fouth-order dispersion and gain terms, a. k. a., the quintic complex Swift-Hohenberg equation, is investgated. The effects of the fourth-order terms to the modulational instability is studied. We numerically investigate the dynamics of the modulational instability in the presence of the fourth-order dispersion and gain terms. – PACS numbers: 42.65.Tg, 42.81DP, 42.65Sf

Key words: Quintic Complex Swift-Hohenberg Equation; Modulation Instability; Optical Gain; Optical Solitary-wave; Numeric Simulation.

1. Introduction

It is well known that a continuous-wave (CW) or quasi-CW radiation propagating in a nonlinear dispersive medium may suffer an instability with respect to weak periodic modulations of the steady state and results in the breakup of the wave into a train of ultrashort pulses [1]. Modulational instability (MI), occuring as a result of an interplay between nonlinearity and dispersion (or diffraction, in the spatial domain), is a fundamental and ubiquitous process that appears in most nonlinear wave systems in nature such as fluid dynamics [2, 3], nonlinear optics [4, 5], and plasma physics [6]. In the context of fiber optics, the temporal MI has been experimentally verified for a single pump wave propagating in a standard nonbirefringence fiber, which can be modeled by the nonlinear Schrödinger (NLS) equation, and it was found that the MI only occurs in anomalous group-velocity dispersion (GVD) regime with a positive cubic nonlinear term [7].

Recently, Hong [8] has investigated the MI of optical waves in a high dispersive cubic-quintic higher-order nonlinear Schödinger equation. In the more complicated optical systems with gain and loss terms, described by the cubic-quintic complex Ginzburg-Landau equation (CGLE), the MI of continuous-waves of the cubic-quintic CGLE has been investigated: the low-amplitude CW solutions are always unstable, while for higher-amplitude CW solutions there are regions of stability and regions where they are modulationally unstable [9].

In this paper, we investigate the properties of the MI of the extended CGLE with fourth-order dispersive terms, a. k. a, *the normalized quintic complex Swift-Hohenberg equation (qCSHE),* which has many important applications in nonlinear optics and complicated pattern-forming dissipative systems, in the form [10 – 12]

$$i\psi z + \frac{D}{2}\psi_{\tau\tau} + |\psi|^2\psi + (h+is)\psi_{\tau\tau\tau\tau} + (\nu - i\mu)|\psi|^4\psi = i\delta\psi + i\beta\psi_{\tau\tau} + i\epsilon|\psi|^2\psi. \quad (1)$$

In mode-locked laser applications, $\psi(z,\tau)$ is the normalized amplitude, z is the propagation distance or the cavity round-trip number (treated as a continuous variable), τ is the retarded time, D is the group-velocity dispersion coefficient with $D = \pm 1$ depending on anomalous ($D = 1$) or normal ($D = -1$) dispersion, h is the fourth-order dispersion, δ the linear gain or loss coefficient, β accounts for spectral filtering or linear parabolic gain ($\beta > 0$) due to an amplifier, the ϵ term represents the nonlinear gain (which arises, e.g., from saturable absorption), the term with μ represents, if negative, the saturation of the nonlinear gain, and the one with ν corresponds, also if negative to the saturation of the nonlinear refractive index, and finally s rep-

0932–0784 / 04 / 0700–0437 $ 06.00

resents the fourth-order correction of the band-limited gain term, i. e., $\beta\psi_{\tau\tau}$ [9, 12].

The analytic solutions of (1) such as bright, black, chirped bright, and chirped black solitary-waves have recently been obtained by using Painlevé analysis, the Hirota multi-linear method and a direct ansatz technique under certain constraints between the coefficients [12, 13]. For the CGLE, intensive researches have previously been performed for finding all analytic and numerical soliton solutions and its dynamical behavior using numerical simulations [9]. However, a detailed analysis of the MI gain spectrum and the evolution of the MI for the qCSHE has not previously been studied and will be pursued in the present work.

The paper is organized as follows. In Sect. 2, we obtain the analytic expression for the MI gain spectrum of the qCSHE, study the characteristics of gain in the presence of the fourth-order dispersion and gain terms, and compare them with those of the CGLE [9]. In Sect. 3, we numerically investigate the dynamics of the initial steady CW in the anomalous regime under a weak modulational field. In particular, the effect of the fourth-order dispersion and gain terms on the final state of the MI (solitary-waves) is investigated. The conclusions follow in Sect. 4.

2. Linear-stability Analysis of Modulational Instability

In order to investigate how weak and time-dependent perturbations evolve along the optical medium described by the qCSHE, we consider the following linear-stability analysis. The steady-state solution of (1) can be given by [1, 8]

$$\bar{\psi}(z,\tau) = A\exp[i\psi_{\mathrm{NL}}(z)], \tag{2}$$

where the linear phase shift $\psi_{\mathrm{NL}}(z)$ is related to the optical amplitude A and the propagation distance z as

$$\psi_{\mathrm{NL}}(z) = zA^2 + z\nu A^4 + i(-z\delta - z\epsilon A^2 - z\mu A^4). \tag{3}$$

The linear-stability of the steady-state can be examined by introducing a perturbed field of the form

$$\begin{aligned}\psi(z,\tau) = [A+\eta(z,t)]\exp[(\delta+\epsilon A^2+\mu A^4)z \\ +\ i(A^2+\nu A^4)z],\end{aligned} \tag{4}$$

where the complex field $|\eta(z,\tau)| \ll A$. It is obvious that, depending on the strength and sign of the gain or loss terms, i. e. δ, ϵ, and μ, the steady-state can blow up or decay. However, due to the presence of the perturbed field and its compensation with the steady-state field, one can expect the total field of (4) to be stable and produce non-trivial coherent structures such as solitary-waves, which will be numerically verified in the following section.

By substituting (4) into (1) and collecting the linear terms in η, we obtain the equation for the perturbed field as

$$\begin{aligned}i\eta_z + \left(\frac{D}{2} - i\beta\right)\eta_{\tau\tau} + (h+is)\eta_{\tau\tau\tau\tau} \\ +\ [(i+2\nu) - i(\epsilon+2\mu)](\eta+\eta^*) = 0,\end{aligned} \tag{5}$$

where * denotes complex conjugate. We assume a general solution of the form

$$\begin{aligned}\eta(z,\tau) = U\exp[i(Kz-\Omega\tau)] \\ +\ V\exp[-i(Kz-\Omega\tau)],\end{aligned} \tag{6}$$

where K and Ω represent the wave number and the frequency of the modulation [1], respectively. Inserting (6) into (5), we obtain the determinant

$$\begin{vmatrix} \Phi^- & \Phi^+ \\ -s\Omega^4 - \beta\Omega^2 + i(-K - \frac{1}{2}d\Omega^2 + h\Omega^4) & s\Omega^4 + \beta\Omega^2 + i(-K + \frac{1}{2}d\Omega^2 - h\Omega^4) \end{vmatrix} = 0, \tag{7}$$

where

$$\begin{aligned}\Phi^{\pm} = \pm K + 2A^2 - d\Omega^2 + h\Omega^4 + 4\nu A^4 \\ +\ i(-2\epsilon A^2 - 4\mu A^4 + \beta\Omega^2 + s\Omega^4).\end{aligned} \tag{8}$$

This results in the expression

$$K = i\sqrt{K_r + iK_i}, \tag{9}$$

for the wave number K, where

$$\begin{aligned}K_r = (s^2-h^2)\Omega^{10} + (2\beta s + Dh)\Omega^8 \\ +\ \Big(\beta^2 - \frac{1}{4}D^2 - 4\mu A^4 s - 4\nu A^6 h \\ -\ 2\epsilon A^2 s - 2A^2 h\Big)\Omega^6\end{aligned}$$

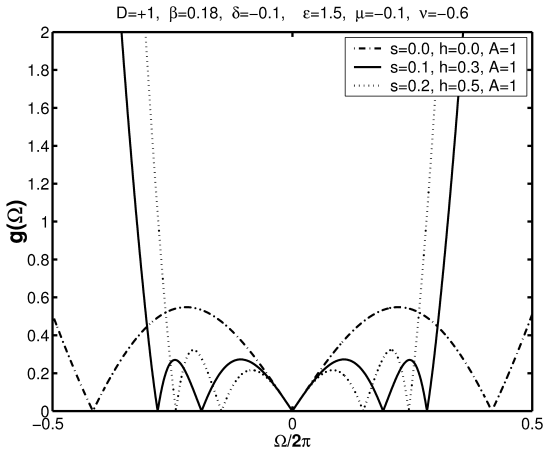

Fig. 1. The gain spectrum of the CGLE (dot-dashed curve) shows two characteristic peaks, while those of the qCSHE (solid and dashed curves) show four peaks due to the functional dependence of Ω, i.e., $g(\Omega) \sim \Omega^5$. The peak frequency, at which the characteristic gain peaks occur, is shown to decrease as s and h increase. However, the gain rapidly increases regardless of the strength of h and s as the modulation frequency increases.

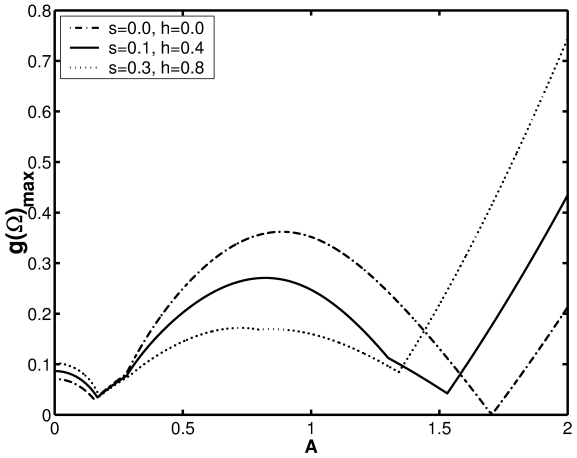

Fig. 2. The maximum gain peaks $g(\Omega)_{\max}$ as a functions of the amplitude A for the same coefficients as in Fig. 1 with several different h and s values in the range of $|\Omega/2\pi| < 0.3$. Nonzero $g_{\max}$ occurs at a much lower amplitude than in the CGLE case. Note that at the higher amplitude around $1.5 < A < 1.7$, there is a region in the model coefficients space where a CW can be stable under MI even in the presence of the fourth-order dispersion terms, since $g_{\max}$ is close to zero.

$$
\begin{aligned}
&+ (-4\mu A^4\beta + 2\nu A^4 D + A^2 D - 2A^2\beta)\Omega^2, \\
K_i = &-2sh\Omega^{10} + (-2h\beta + Ds)\Omega^8 + (4\mu A^4 h \\
&- 4\nu A^4 s + 2\epsilon A^2 h + D\beta - 2A^2 s)\Omega^6 \\
&- (4\nu A^4\beta + \epsilon A^2 D + 2\mu A^4 D + 2A^2\beta)\Omega^2.
\end{aligned} \tag{10}
$$

Expressing (9) in polar coordinates, we obtain

$$
\begin{aligned}
K &= i[K_r^2 + K_i^2]^{1/4}\left[\cos\left(\frac{\theta}{2}\right) + i\sin\left(\frac{\theta}{2}\right)\right] \\
&= \frac{i}{2}[K_r^2 + K_i^2]^{1/4}[\sqrt{2 + 2\cos(\theta)} \\
&\quad + i\sqrt{2 - 2\cos(\theta)}],
\end{aligned} \tag{11}
$$

where $\cos(\theta) = K_r/\sqrt{K_r^2 + K_i^2}$. The steady-state solution becomes unstable whenever K has an imaginary part since the perturbation then grows exponentially with the intensity given by the MI gain defined as $g(\Omega) \equiv 2\mathrm{Im}(K)$ [1] as

$$
\begin{aligned}
g(\Omega) &= [K_r^2 + K_i^2]^{1/4}\sqrt{2 + 2\cos(\theta)} \\
&= [2\sqrt{K_r^2 + K_i^2} + 2K_r]^{1/2}.
\end{aligned} \tag{12}
$$

The inclusion of the fourth-order dispersion and gain terms lets the MI gain spectrum depend on higher modulation frequencies, i.e., $g(\Omega) \sim \Omega^5$ instead of $g(\Omega) \sim \Omega^3$ for the CGLE in [9]. Thus, the gain spectrum of (12) grows indefinitely as the modulation frequency increases even for small h and s values. However, at small modulation frequencies the lower orders of the Ω terms of K_r and K_i dominate over the highest order Ω. Thus we expect that the characteristic MI gain peaks occur as in [1, 8].

Figure 1 shows the MI gain spectrum $g(\Omega)$ as function of $\Omega/2\pi$ for several values of h, s, and the optical amplitude A with the following set of physical coefficients used in [9]: $\beta = 0.18, \delta = -0.1, \mu = -0.1, \nu = -0.6$, and $\epsilon = 1.5$. In case of the CGLE (dot-dashed curve), i. e., $h = s = 0$, there are two local peaks at low modulational frequencies ($|\Omega/2\pi| < 0.5$). However, the gain spectra of the qCSHE (solid and dashed curves) show four characteristic peaks appearing at the low frequencies $|\Omega/2\pi| < 0.3$, rapidly increasing at $|\Omega/2\pi| > 0.3$. As mentioned above, it can be seen from Fig. 1 that the overall effect of the fourth-order dispersion and gain terms to the MI gain is to make the spectrum narrower as the values increase.

Figure 2 shows the dependence of the maximum gain peak $g(\Omega)_{\max}$ on A, using the same coefficients as in Fig. 1, for the modulation frequency in the range $|\Omega/2\pi| < 0.3$. Comparing with the maximum gain peak of the CGLE (dot-dashed curve), those of

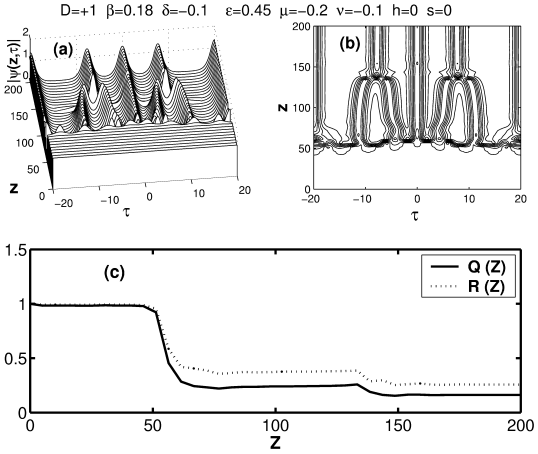

Fig. 3. (a) Simulation of an injected CW to the nonlinear medium supporting anomalous dispersion with $\Omega_m = 0.001$ and $\epsilon_m = 0.01$, which qualitatively agrees with the result in [9]. The initial CW transforms to solitary-waves after interaction. Note that the solitary-wave located in the center is directly generated by the initial modulated field, (b) Contour plot of (a). (c) The evolution of normalized energy and mass $Q(z)$ and $R(z)$, respectively. $Q(z)$ is almost constant up to $z \cong 50$ and thereafter drops to 30% of the initial value, since the nonlinear terms (δ, ϵ, $\mu < 0$) in (1) act as an effective energy loss.

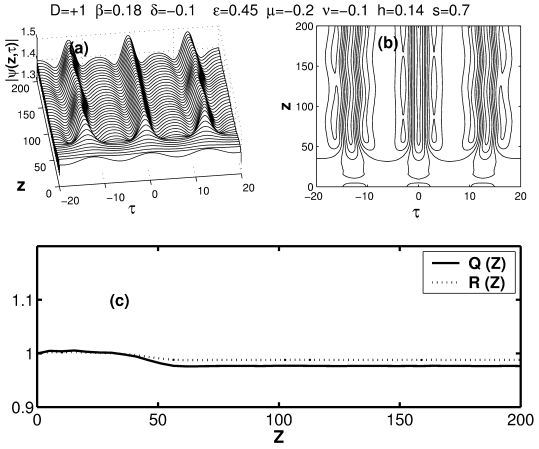

Fig. 4. The evolution of the initial CW with $\Omega_m = 0.5$ and $\epsilon_m = 0.001$. (a) The presence of fourth-order dispersion and gain terms give rise to a 'breathing' and 'creeping' motion of the waves along the evolution distance. (b) The contour plot shows that the solitary-wave in the center is stationary. (c) Evolution of $Q(z)$ and $R(z)$ with the fourth-order terms, which shows a slight variation of their initial values, indicating their role as energy supplier to the system.

the qCSHE (solid and dashed curves) in Fig. 2 show nonzero gain maxima at much lower amplitude. On the other hand, for $1.5 < A < 1.7$, there is a region of the model coefficients where the CW can be stable under the MI even in the presence of the fourth-order dispersion and gain terms, since $g_{\max}$ is close to zero.

Before we proceed to the numerical simulations of the MI, it is worth noting that the wave number K in (11) has not only the purely growing imaginary term but also the real term, giving an oscillatory instability which may influence to a solitary-wave formation at the end process of the MI. As shown in (4), the exponentially decaying ($\delta < 0$, $\epsilon < 0$, and $\mu < 0$ in this work) or increasing factor can modify (12), therefore the effective gain is given as

$$g_{eff}(\Omega) = (\delta + \epsilon A^2 + \mu A^4) + \left[2\sqrt{K_r^2 + K_i^2} + 2K_r\right]^{1/2}, \quad (13)$$

which only shifts the magnitude of (12).

3. Numerical Simulations

In order to understand the dynamics of a CW under the MI, (1) is solved, utilizing the split-step Fourier method applying the periodic boundary condition [14]. We use an incident field at the launch plane $z = 0$ into the nonlinear medium of the form

$$\psi(0, \tau) = [A + \epsilon_m \cos(\Omega_m \tau)], \quad (14)$$

where ϵ_m is the strength of the modulation amplitude and Ω_m is the angular frequency of a weak sinusoidal modulation imposed on the CW, which can be determined from the gain spectra for the given set of coefficients, such as Figure 1. Among many sets of possible coefficients of (1), in this section we only focus on the effects of the h and s terms to the evolution of the MI.

In Fig. 3, we present the simulation of an injected CW to the nonlinear medium supporting anomalous dispersion ($D = 1$) by choosing, as an example, $\beta = 0.18$, $\delta = -0.1$, $\mu = -0.2$, $\nu = -0.1$, and $\epsilon = 0.45$, using the same set of coefficients in Fig. 1 (dot-dash curve), and applying the modulation frequency $\Omega_m = 0.001$ with a perturbed field amplitude $\epsilon_m = 0.01$. Figures 3a,b show the occurrence of several modulation fields which in turn generate the solitary-waves due to the MI. In particular, the solitary-wave located in the center of Fig. 3a is directly generated from the initial modulated field, which is different from the result in [9], where the solitary-waves can be produced only through the interaction of initial perturbed fields. The dynamical properties of the MI and the evolution

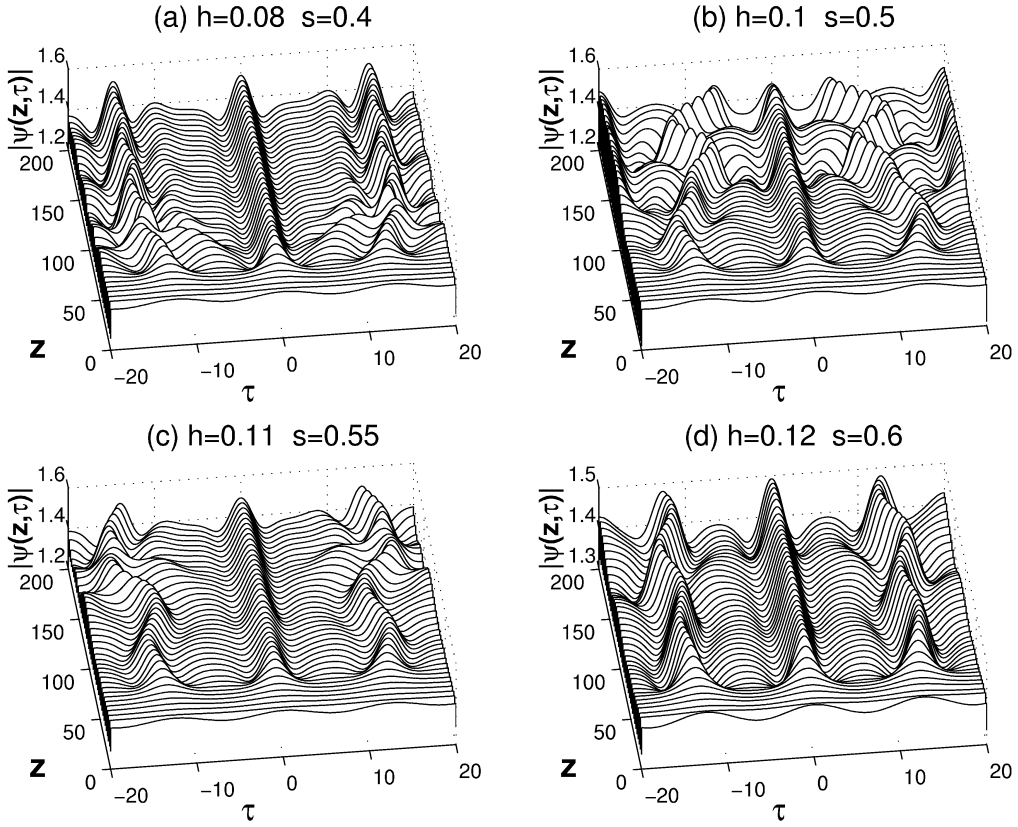

Fig. 5. The effect of the fourth-order terms to the MI with the same set of coefficients as for Fig. 3 and increasing strength of h and s: (a) $h = 0.08$ and $s = 0.40$; (b) $h = 0.10$ and $s = 0.50$; (c) $h = 0.11$ and $s = 0.55$; (d) $h = 0.12$ and $s = 0.60$. The breathing and creeping behaviors of the solitary-waves are more conspicuous if the strength increases.

of solitary-waves can be more throughly investigated from the energy and mass (or the area under $|\psi(z,\tau)|$) defined as

$$\varepsilon(z) \equiv \int_{-\infty}^{\infty} |\psi(z,\tau)|^2 \mathrm{d}\tau, \qquad M(z) \equiv \int_{-\infty}^{\infty} |\psi(z,\tau)| \mathrm{d}\tau, \tag{15}$$

respectively. Figure 3c shows the evolution of the normalized energy $Q(z) \equiv \varepsilon(z)/\varepsilon(0)$ and the normalized mass $R(z) \equiv M(z)/M(0)$, respectively, where the energy Q(z) of the system is almost constant up to $z \cong 50$ and thereafter drops to 30% of the initial value, since the nonlinear terms (δ, ϵ, $\mu < 0$) in (1) in this case act as an effective energy loss. Also, it is shown that the solitary-waves are produced at $z \cong 60$ due to the MI. At $z \cong 145$ the collision of two solitary-waves occurs, and $Q(z)$ and $R(z)$ decrease as before. It has been checked through several numerical simulations that the solitary-waves are maintained in stationary motion and the energy is conserved up to $z = 1000$.

In Fig. 4, for example, the effect of the fourth-order dispersion and gain terms to the evolution of MI is investigated for $h = 0.14$, $s = 0.7$, $\epsilon_m = 0.01$, and $\Omega_m = 0.5$ with the same coefficients as in Figure 3. Contrary to the stable evolution of the solitary-waves in Fig. 3a, the presence of those terms give rise to a 'breathing' and 'creeping' motion of the waves along the evolution distance. It is seen from Fig. 4a that the solitary-wave in the center shows a stationary motion similar to that of Figs. 3a and 3b, but the other waves both breathe and creep during their propagation, which is clearly observed in the contour plot of Fig. 4b. $Q(z)$ and $R(z)$ calculated in Fig. 4c shows a slight decrease from their initial values in comparison with those of Fig. 3c, which indicates that they compensate the loss due to the nonlinear terms of (1) by providing energy to the system.

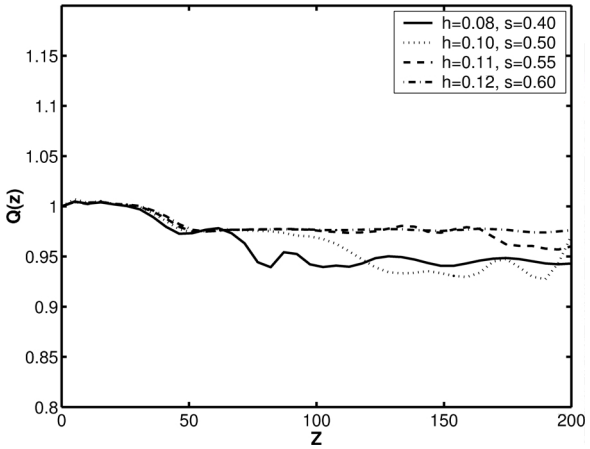

Fig. 6. The evolution of $Q(z)$ with that of the fourth-order dispersion and gain terms. The energy, as expected, is shown to become more stable as the strength of the fourth-order terms increases.

Finally, in Fig. 5 we further investigate the dynamics of the MI under the fourth-order terms with increasing strength: (a) $h = 0.08$ and $s = 0.40$; (b) $h = 0.10$ and $s = 0.50$; (c) $h = 0.11$ and $s = 0.55$; (d) $h = 0.12$ and $s = 0.60$. The simulation result in Fig. 5 shows that the breathing and creeping behaviors of the solitary-waves are more conspicuous as the strength of the coefficients increases. In particular, the creeping solitary-waves in Fig. 5b interact with the center wave so that it breathes more violently during the evolution. On the other hand, the energy in Fig. 6, as expected, is shown to be the more stable the more the strength increases.

4. Conclusions

In this work we have derived the analytic expression for the MI gain of the qCSHE in (1), which is an extended model of the cubic-quintic complex Ginzburg-Landau equation, by adding the fourth-order dispersion and gain terms. It is shown that the presence of fourth-order dispersion and gain terms changes the characteristic MI gain spectrum of the CGLE as shown in Figure 1. The fourth-order terms make the MI gain spectrum depend on a higher modulation frequency, i.e., $g(\Omega) \sim \Omega^5$ in comparison with $g(\Omega) \sim \Omega^3$ for the case of CGLE in [9]. The maximum gain spectra shown in Fig. 2 are different from those of [9], in that all CWs for the given particular set of coefficients are unstable. Using the split-step Fourier method, we numerically demonstrated the dynamics of the CW in the presence of fourth-order dispersion and gain terms in Figures 4 – 6. The terms give rise to 'breathing' and 'creeping' motion of the waves along the evolution distance, as shown in Figs. 4a and 5. On the other hand, their effect on $Q(z)$ and $R(z)$ has been calculated in Fig. 4c, showing a slight decrease from their initial values in comparison with those of Fig. 3c, which indicates that they compensate the loss due to the nonlinear terms (δ, ϵ, $\mu < 0$) in (1) by providing energy to the system.

Acknowledgements

This work was supported by the Korean Research Foundation, Grant No. 2002-015-CP0135. The author gratefully acknowledges Prof. A. Ng for warm hospitality while visiting the University of British Columbia.

[1] G. P. Agrawal, Nonlinear Fiber Optics, Optics and Photonics, Academic Press, 2001.
[2] G. B. Whitham, Proc. Roy. Soc. London **283**, 238 (1965).
[3] T. B. Benjamin and J. E. Feir, J. Fluid Mech. **27**, 417 (1967).
[4] V. I. Bespalov and V. I. Talanov, JETP Lett. **3**, 307 (1966).
[5] V. I. Karpman, JETP Lett. **6**, 277 (1967).
[6] T. Taniuti and H. Washimi, Phys. Rev. Lett. **21**, 209 (1968).
[7] K. Tai, A. Hasegawa, and A. Tomita, Phys. Rev. Lett. **56**, 135 (1986).
[8] W. P. Hong, Optics Commun. **213**, 178 (2002).
[9] J. M. Soto-Crespo, N. Ahkmediev, and G. Town, J. Opt. Soc. Amer. B. **19**, 234 (2002).
[10] M. C. Cross and P. C. Hohenberg, Rev. Mod. Phys. **65**, 851 (1993).
[11] H. Sakaguchi and H. R. Brand, Physica D **117**, 95 (1998).
[12] A. Ankiewicz, K. Maruno, and N. N. Akhmediev, preprint-02090552 (2002).
[13] K. I. Maruno, A. Ankiewicz, and N. Akhmediev, preprint-0209045 (2002).
[14] J. A. C. Heideman and B. M. Herbst, SIAM J. Numer. Anal. **23**, 485 (1986).